Proximate determinants of bite force in *Anolis* lizards

Antoine Wittorski,[1] Jonathan B. Losos[2] and Anthony Herrel[1,3]

[1]*Département d'Ecologie et de Gestion de la Biodiversité, UMR 7179 C.N.R.S/M.N.H.N., Paris, France*
[2]*Department of Organismic and Evolutionary Biology, Harvard University, Cambridge, MA, USA*
[3]*Evolutionary Morphology of Vertebrates, Ghent University, Ghent, Belgium*

Abstract

Performance measures associated with the vertebrate jaw system may provide important insights into vertebrate ecology and evolution because of their importance in many ecologically relevant tasks. Previous studies have shown that in many taxa, evolution toward higher bite force has gone hand in hand with the evolution of larger body size. However, independent of differences in overall body size, bite force may vary depending on head size and shape as well. Moreover, the underlying musculature may also drive variation in bite force. Here, we investigate the proximate determinants of bite force in lizards of the genus *Anolis*. We dissected the jaw muscles and quantified muscle mass, fibre length, and cross-sectional area. Data were analysed for both sexes independently given the sexual dimorphism detected in the dataset. Our results show that the traits that explain bite force are similar in both males and females with overall body size and muscle mass being the principal determinants. Among the different muscles examined, the adductor externus and the pseudotemporalis groups were the best determinants of bite force. However, models run for males predicted the variation in bite force better than models for females, suggesting that selection on morphology improving bite force may be stronger in males.

Key words: muscle; head shape; biting; sexual dimorphism.

Introduction

Performance, or the ability of an animal to execute an ecologically relevant task (Huey & Stevenson, 1979), is commonly measured in ecomorphological studies as it is thought to be a good proxy for fitness. Performance measures associated with the vertebrate jaw system provide important insights into vertebrate ecology and evolution given their importance in many ecologically relevant tasks (Herrel et al. 2007b). In vertebrates, bite force is an important performance trait due to its direct link to many functions, including feeding behaviour (Herrel et al. 2001b; Herrel & O'Reilly, 2006; Herrel & Holanova, 2008), reproduction and mating (Anderson & Vitt, 1990; Herrel et al. 1996, 2009; Lappin & Husak, 2005; Chazeau et al. 2013), agonistic and territorial behaviour (Cooper & Vitt, 1993; Lailvaux et al. 2004), and defence against predators (Leal & Rodríguez-Robles, 1995), all of which impact an individual's fitness. Thus, bite force can be used as a fitness-relevant whole-organism performance measure (Anderson et al. 2008).

Previous studies have shown that in many taxa, evolution toward higher bite force has gone hand in hand with the evolution of larger body size (Aguirre et al. 2002; Herrel et al. 2004, 2010; Chazeau et al. 2013). However, independent of differences in overall body size, differences in bite force are often observed and thought to be due to differences in overall head size (Herrel et al. 2001a, 2006). Having a bigger head would result in a larger absolute jaw muscle volume, all else being equal, conferring a bite performance advantage (Herrel et al. 2001a, b). Nevertheless, growing a relative larger head may trade off with other functions (e.g. the ability to hide in crevices, burrowing, climbing ability; see Herrel et al. 2001a; Kohlsdorf et al. 2008; Barros et al. 2011) and may thus not always be possible. Consequently, not only relative head size but also head shape can be an important determinant of bite force (Herrel et al. 2007a; Fabre et al. 2014a,b). Differently shaped heads allow for variation in muscle arrangement, pennation angle, and muscle mass, which in turn may impact bite force (Herrel et al. 2001a, 2006; Lappin et al. 2006). Moreover, in comparisons among some lizard species, differences in bite force cannot be accounted for solely by differences in head size, which suggests that differences in the underlying musculature may also play a role (Herrel et al. 1999). Head shape varies in a complex and multivariate way, suggesting that there may be more than one way to increase

Correspondence

Anthony Herrel, UMR 7179 C.N.R.S/M.N.H.N., 55 rue Buffon, 75005 Paris, France. T: + 33 1 40798120; E: anthony.herrel@mnhn.fr

bite force (Harmon et al. 2005). Untangling the evolutionary drivers behind differences in bite force is consequently difficult.

Here, we investigate the proximate determinants of bite force in lizards of the genus *Anolis*. We chose this genus because it is species-rich and morphologically diverse (Williams, 1983; Losos et al. 1998; Jackman et al. 1999; Pinto et al. 2008; Sanger et al. 2008; Nicholson et al. 2012). Moreover, the sexes of most anole species are dimorphic in head size (Butler & Losos, 2002; Irschick et al. 2005; Herrel et al. 2006, 2007a), leading to interspecific and inter-sexual differences in diet and bite force (Herrel et al. 2004, 2006). Given the different functional requirements of the head in males and females (principally diet in females vs. diet and male–male combat in males; Lailvaux et al. 2004; Herrel & O'Reilly, 2006), the factors determining bite force may not be the same in both sexes. We specifically predict that in males, bite force will be mainly determined by muscles with long fibres that are effective at large gapes, given that (1) males use jaw-locking during male–male combat (Lailvaux et al. 2004), (2) males in some species have differently shaped heads (e.g. Herrel et al. 2007a), and (3) males typically eat larger and harder prey than females (Herrel et al. 2006).

Material and methods

Specimens

In this study, 48 specimens of the genus *Anolis* belonging to 15 species were used (Fig. 1). Specimens from the collections of the Museum of Comparative Zoology at Harvard University (Supporting Information Table S1) and from the personal collection of Anthony Herrel were used for dissection. Species were selected to represent a diversity of ecologies and morphologies. For each species we selected between three and five adults representing both sexes based on their availability (except for *Anolis pentaprion*, for which only one specimen was available for dissection). Adults were identified as being reproductively active with fully developed gonads. Both males and females were included in the analysis.

Dissection and muscle properties

All specimens used for the analysis were stored in a 70% aqueous ethanol solution. Before dissection each specimen was submerged in water for 15 min to rehydrate it. The nomenclature of Haas (1973) is used for all muscles (see Supporting Information Table S2). Jaw muscles were removed unilaterally on each specimen using a dissecting microscope (Wild M3Z, Wild Inc., Heerbrugg, Switzerland). Next, muscles were weighed using a digital scale (Mettler type AE100; Mettler-Toledo GmbH, Giessen, Switzerland; precision: 0.0001 g). Next, fibre lengths were obtained by submerging the muscles in a 30% nitric acid (HNO_3 30%) solution for 24 h to dissolve all connective tissue. Muscle fibres were then put in a 50% glycerol solution and the average fibre length of each muscle was determined by drawing at least five fibres for every muscle (using a dissecting microscope with *camera lucida*). Drawings were scanned and fibre lengths were quantified using IMAGEJ 1.47v (Wayne Ras-

band, National Institutes of Health, Bethesda, MD, USA). Next we calculated the average length of the fibres for each muscle. Finally, the physiological cross-sectional area (PCSA) of each muscle was calculated as follows:

$$PCSA = \frac{mass\,(g)/muscular\ density\left(\frac{g}{cm^3}\right)}{fibre\ length\,(cm)}.$$

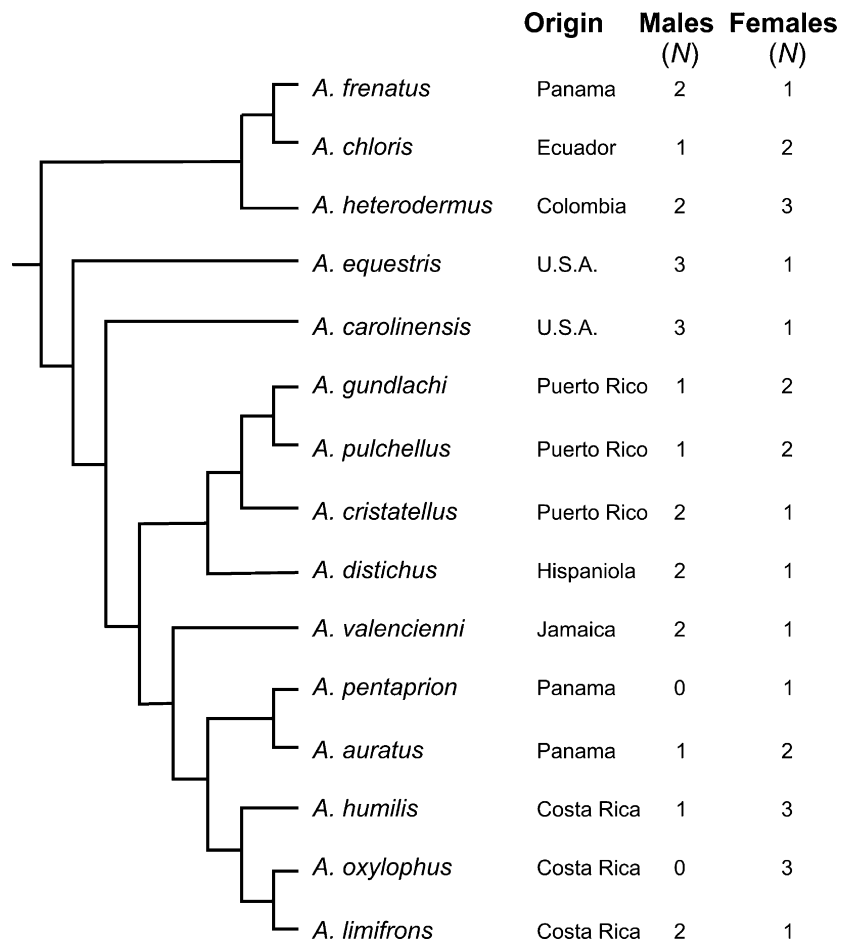A muscular density of 1.06 g cm^{-3} (Mendez & Keys, 1960) was used.

Head dimensions

Seven morphological measurements were taken for all specimens before dissection (Supporting Information Table S3, Fig. 2). We used the same measurements as described in Herrel & Holanova (2008). Snout–vent length (SVL) was measured from the tip of the snout to the posterior edge of the anal scale, head length (headl) from the back of the parietal bone to the tip of the upper jaw, head width (headw) at the widest part of the head (at the level of jugal bones), head height (headh) at the highest part of the head (posterior to the orbits), lower jaw length (lower jawl) from the back of the retroarticular process to the tip of lower jaw, snout length (tip-coron) from the tip of the lower jaw to the posterior edge of the jugal (as an indicator of the position of the coronoid), and jaw outlever (tip-quadr) from the tip of the lower jaw to the anterior edge of the ear opening (corresponding to the posterior edge of the quadrate). Both lower jaw length and the distance from the tip of the jaw to the coronoid reflect the biomechanics of the jaw system. By subtracting 'tip-coron' from 'tip-quadr' we calculated the length of the jaw closing inlever; by subtracting 'tip-quadr' from 'lower jawl' we calculated the jaw opening inlever. All measurements were taken using digital callipers (Mitutoyo CD-20DC, Kawasaki, Japan; precision: 0.01 mm), and were taken on the left side of the specimens whenever possible. If measurements could not be taken on the left side because the head was damaged, then measurements were taken on the right side.
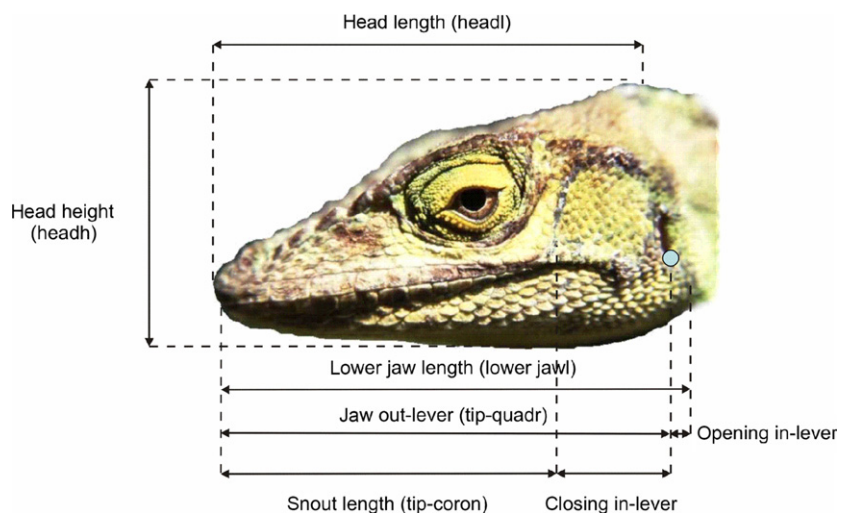
Bite force

In vivo bite forces were measured in the field (Supporting Information Table S4). Data were obtained for *Anolis oxylophus*, *Anolis humilis* and *Anolis limifrons* at La Selva, Costa Rica, in 2008; for *Anolis frenatus*, *Anolis auratus* and *Anolis pentaprion* in Gamboa, Panama, in 2009; for *Anolis chloris* in Otongachi, Ecuador, in 2010; for *A. heterodermus* in Bogota, Colombia, in 2013; for *Anolis equestris* in Florida, in 2003; for *Anolis carolinensis* near New Orleans, in 2003; for *Anolis cristatellus*, *Anolis gundlachi* and *Anolis pulchellus* near El Yunque, Puerto-Rico, in 2004; for *Anolis valencienni* at Discovery Bay, Jamaica, in 2003; and for *Anolis distichus* near the Barahona peninsula in the Dominican Republic in 2004 (see also Herrel et al. 2004; Vanhooydonck et al. 2005a,b; Munoz et al. 2015). Only data for adult males and females were used in this study so they could be compared with muscle data obtained through dissection for individuals of similar size (see Tables S3 and S4).

Bite forces were measured using an isometric Kistler force transducer (type 9203, range 7500 N; Kistler, Zurich, Switzerland) mounted on a purpose-built holder and connected to a Kistler charge amplifier (type 5995A, Kistler; see Herrel et al. 1999 for a more detailed description of the setup). When the bite plates were placed between the jaws of the animal, prolonged and repeated

	Origin	Males (N)	Females (N)
A. frenatus	Panama	2	1
A. chloris	Ecuador	1	2
A. heterodermus	Colombia	2	3
A. equestris	U.S.A.	3	1
A. carolinensis	U.S.A.	3	1
A. gundlachi	Puerto Rico	1	2
A. pulchellus	Puerto Rico	1	2
A. cristatellus	Puerto Rico	2	1
A. distichus	Hispaniola	2	1
A. valencienni	Jamaica	2	1
A. pentaprion	Panama	0	1
A. auratus	Panama	1	2
A. humilis	Costa Rica	1	3
A. oxylophus	Costa Rica	0	3
A. limifrons	Costa Rica	2	1

Fig. 1 Composite phylogeny representing the relationships between the species included in the comparative analysis; modified from Castaneda & De Queiroz (2013) and Nicholson et al. (2012). All branch lengths are set to unity. The geographic origin of the specimens and the number of females and males dissected for each species are indicated.

Fig. 2 Illustration of the measurements taken of the heads of the lizards. Note that head width is not illustrated here. Modified after Herrel & Holanova (2008).

biting resulted. The place of application of bite forces was standardized for all animals by metal stops that were mounted on the bite plates, thus assuring that animals always bit at the same position along the jaw. Gape angle was standardized by moving the bite plates away from each other for larger animals. Measurements were repeated five times for each animal, with an inter-trial interval of at least 30 min. The maximal value obtained during such a recording session was considered to be the maximal bite force for that individual.

Statistical analyses

All muscular and morphological variables were logarithmically transformed ($\log_{10}$) before the analysis to fulfil assumptions of nor-

mality and homoscedasticity. We first tested for dimorphism in the different traits using paired-sample *t*-tests on the log$_{10}$-transformed means of the original variables. As sexual dimorphism was significant (see also Butler & Losos, 2002; Herrel et al. 2006, 2007a), we ran all subsequent analyses for males and females separately.

Species are not independent data points and as such, phylogeny needs to be taken into account in the analyses (Felsenstein, 1985). To test for phylogenetic signal in the data, a univariate lambda (Ives et al. 2007) was calculated on the log-transformed means of the raw data for males and females separately using the phylosig function in the phytools library (Revell, 2012) in R (R Core Team, 2014). To do so, a composite tree was constructed depicting the relationships between the species in our analysis by combining trees from the literature (Nicholson et al. 2012; Castaneda & De Queiroz, 2013) (Fig. 1). This tree should be considered an estimate of the relationships between species only. As few data are available for the divergence times between species, we set all branch lengths to unity (see Martins & Garland, 1991). All trait values were input at the tree tips, allowing us to calculate phylogenetic independent contrasts of each variable using the PHENOTYPIC DIVERSITY ANALYSIS PROGRAM (PDAP). Inspection of the diagnostic graphs and statistics in the MESQUITE program was performed (Maddison WP, Maddison DR 2011. Mesquite: a modular system for evolutionary analysis. Version 2.75) allowing us to verify that branch lengths were indeed adequate for the analysis of all variables. If not, branch lengths set to unit length were transformed using the 'branch lengths method of Nee' and 'Grafen's Rho transformations' (Rho = 0) (Grafen, 1989; Díaz-Uriarte & Garland, 1998).

To investigate the effect of head dimensions and muscle characteristics on bite performance we proceeded as follows: first we ran factor analyses with varimax rotation on the independent contrasts of the head measurements and extracted two factors. Next we ran a factor analysis with varimax rotation on the independent contrasts of the muscle mass data and also extracted the first two factors. Finally, we ran a factor analysis with varimax rotation on the independent contrasts of fibre length and extracted the first two factors. Next, we ran a multiple regression with bite performance as the dependent variable and the six factors summarizing variation in head morphology, muscle mass and muscle fibre length as independent variables. To do so we used the morphological data measured on the specimens and the bite forces measured in the field. To assess which variables determined most strongly variation in bite force we examined the standardized partial regression coefficients.

In a second analysis, the mass and physiological cross-sectional area of the jaw muscles were combined into three major functional groups: the adductor mandibulae (LAO, AMESA, AMESP, AMP, AMEP), the pseudotemporalis (PSTS, PSTP) and the pterygoideus (PTL, PTM) (Herrel et al. 1998). Next, we calculated the independent contrasts for these variables as described above and used these as input for a multiple regression with the independent contrasts of bite performance as the dependent variable and the muscular traits as independent variables.

Results

Morphology

In the following descriptions, the muscle nomenclature of Haas (1973) is used. Jaw muscles are composed of two distinct functional groups. The first group consists of muscles involved in the jaw opening, and the other one includes muscles involved in jaw closing. The *m. cervicomandibularis* (CM) and the *m. depressor mandibulae* (DM) together compose group one. The jaw-closing muscle group is composed of one minor muscle not involved in bite force generation (1m. levator anguli oris) and five major muscle groups:

1 The external adductor complex (MAME), which was further subdivided into three major parts: a superficial part (consisting of an anterior and a posterior part), a medial part and a deep part.
2 The posterior adductor (MAMP).
3 The pseudotemporal complex (MPsT), which consist of two parts, i.e. superficial and deep.
4 The pterygoid group (MPt), which was subdivided into two parts (lateral and medial).
5 The constrictor dorsalis group (MPPt and MLPt). The constrictor dorsalis group consists of the *m. protractor pterygoidei* (MPPt) and the *m. levator pterygoidei* (MLPt).

The different muscle layers are depicted in Fig. 3 (see also Herrel et al. 1998). A brief description of the different muscles is given below.

M. cervicomandibularis (CM) – runs from the dorsal cervical connective tissue sheet and inserts on the postero-ventral side of the retroarticular process. In some specimens the CM is absent.

M. depressor mandibulae (DM) – attaches to the skull and the dorsal connective tissue sheet and runs postero-ventrally to insert on the postero-dorsal side of the retroarticular process.

M. levator anguli oris (LAO) – originates at the ventrolateral side of the junction between the jugal and the squamosal, and the fibres run obliquely to insert at the connective tissue associated with the *anguli oris*. The connective tissue of the *anguli oris* is tightly connected with the jugomandibular ligament, which originates on the articular bone at the level of the quadrate and runs anteriad to attach to the posterior most lateral aspect of the jugal bone.

M. adductor mandibulae externus superficialis anterior (AMESA) – a massive muscle in the genus *Anolis*. The AMESA originates at the inner side of the squamosal, the tip of the quadrate and the parietal bone. The fibres run ventrad and insert at the lateral aspect of the coronoid and the inner side of the angular, anterior to the trigeminal nerve.

M. adductor mandibulae externus posterior (AMESP) – a small muscle compared with the anterior part. The AMESP originates at the anterior side of the quadrate and the fibres run obliquely ventrad to insert at the dorsal aspect of the lower jaw, onto a fossa on the superior side of the angular.

M. adductor mandibulae externus medialis (AMEM) – another large muscle in anoles; this muscle and AMESA constitute the majority of the head muscle
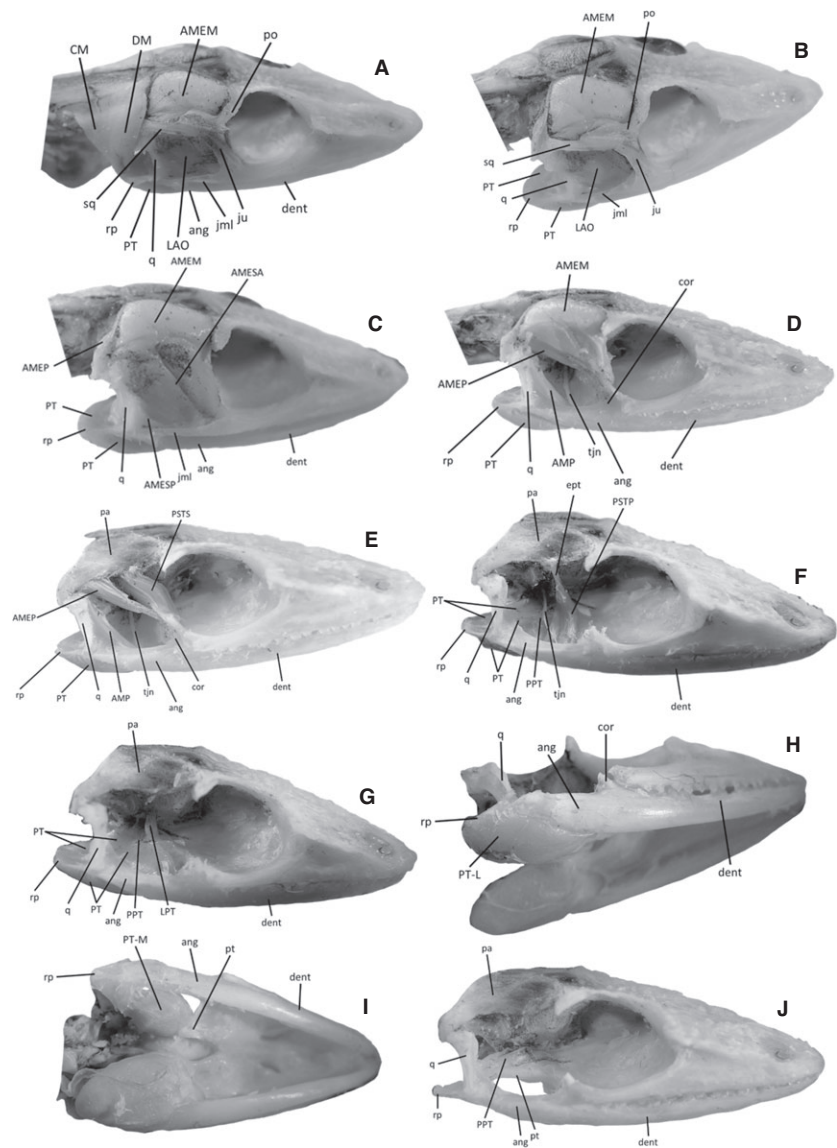
Fig. 3 Illustrations representing the jaw musculature of *Anolis*. (A) Lateral view after removal of the skin; AMEM, m. adductor mandibulae externus medialis; ang, angular; CM, m. cervicomandibularis; dent, dentary; DM, m. depressor mandibulae; LAO, m. levator anguli oris; jml, jugal mandibular ligament; ju, jugal; po, post-orbital; PT, m. pterygoideus; q, quadrate; rp, retroarticular process; sq, squamosal. (B) Lateral view after removal of the CM and DM. (C) Lateral view after removal of the CM, DM, LAO, sq, and a part of the po and ju. AMEP, m. adductor mandibulae externus profondus; AMESA, AMESP, m. adductor mandibulae externus superficialis anterior and posterior. (D) Lateral view after removal of the AMESA and AMESP. AMP, m.adductor mandibulae posterior; cor, coronoid; tjn, nervus trigeminus. (E) Lateral view after removal of the AMEM. pa, parietal; PSTS, m. pseudotemporalis superficialis. (F) Lateral view after removal of the AMEP, AMP and PSTS. ept, epipterygoid; PPT, m. protractor pterygoidei; PSTP, m. pseudotemporalis profondus. (G) Lateral view after removal of the PSTP and ept. LPT, m. levator pterygoidei. (H) Ventral view. PTL, m. pterygoideus pars lateralis. (I) Ventral view after removal of the PTL. pt, pterygoid; PTM, m. pterygoideus pars medialis. (J) Lateral view after removal of the LPT, PTL and PTM.

mass. The fibres of the AMEM originate on the parietal bone and run ventrad to insert at the external sheet of the coronoid aponeurosis, below the AMESA and anterior to the AMEP.

M. adductor mandibulae externus profondus (AMEP) – originates at the dorsal side of the parietal bone and runs throughout the parietal fenestra and inserts at the external sheet of the coronoid aponeurosis, below the AMESA and posterior to the AMEM insertion.

M. adductor mandibulae posterior (AMP) – generally triangular in shape. The AMP originates at the anterior inferior part of the quadrate and runs obliquely forward to insert at the inner side of lower jaw, posterior to the trigeminal nerve.

M. pseudotemporalis superficialis (PSTS) – originates at the ventrolateral aspect of the parietal near the front-parietal suture and at the external side of the

upper half of the epipterygoid. The fibres run almost vertically to insert at the medial sheet of the coronoid aponeurosis at the base of the coronoid.

M. pseudotemporalis profondus (PSTP) – originates at the bottom half of the epipterygoid and the brain case. The fibres run almost vertically alongside the epipterygoid and insert in the interior corner of the mandibular fossa, near the dentary-angular suture.

M. pterygoideus pars lateralis (PTL) – originates tendinously at the ectopterygoid-pterygoid junction, curves around the lower jaw and inserts at the ventro-lateral aspect of the retroarticular process.

M. pterygoideus pars medialis (PTM) – originates at the antero-lateral side of the pterygoid and insert at the medial side of the articular.

M. levator pterygoidei (LPT) – weakly developed muscle originating tendinously at the ventral aspect of

the occipital bone and hidden by the epipterygoid. The fibres run vertically to insert at the dorsal aspect of the pterygoid.

M. protractor pterygoidei (PPT) − originates at the anterior side of the basioccipital bone, runs obliquely posteriad and inserts at the dorsal aspect of the pterygoid bone, posterior to the insertion of the LPT.

Quantitative data on muscle masses and fibre lengths for males and females are provided in Supporting Information Tables S5–S7.

Sexual dimorphism

Most of the variables examined with the exception of the mass and cross-sectional area of the constrictor dorsalis, snout length, and the opening and closing inlever were significantly different between males and females (Table 1).

Phylogenetic signal

Bite force and several morphological traits showed significant phylogenetic signal (Table 1). However, of the muscle traits examined, only the mass of the m. depressor mandibulae in males showed significant phylogenetic signal (Table 1). Unexpectedly, phylogenetic signal was generally stronger for females than for males.

Table 1 Results of the test for sexual dimorphism (paired *t*-test) and the phylogenetic signal (Pagel's lambda) in the data.

Variable	Paired *t*-test P	Males Lambda	P	Females Lambda	P
Bite force	*0.003*	0.59	0.13	**0.91**	**0.004**
SVL	*0.005*	0.51	0.29	**0.95**	**0.014**
Mass depressor	*0.048*	**0.91**	**0.02**	0.79	0.13
Mass adductor	*0.023*	0.7	0.19	0.81	0.17
Mass PsT	*0.047*	0.39	0.57	0.71	0.19
Mass Pterygoidei	*0.020*	0.56	0.5	0.78	0.17
Mass constrictor	0.081	0.64	0.26	0.00007	1
PCSA depressor	*0.011*	0.72	0.31	0.73	0.17
PCSA adductor	*0.004*	0.00004	1	0.91	0.06
PCSA PsT	*0.005*	0.35	0.51	0.65	0.3
PCSA Pterygoidei	*0.032*	0.62	0.45	0.9	0.06
PCSA constrictor	0.057	0.67	0.24	0.00005	1
Head length	*0.011*	0.85	0.15	0.9	0.07
Head width	*0.029*	0.00007	1	0.67	0.3
Head height	*0.004*	0.78	0.24	0.9	0.06
Lower jaw length	*0.015*	0.58	0.43	**0.93**	**0.03**
Outlever	*0.022*	0.56	0.4	**0.92**	**0.04**
Snout length	0.079	0.73	0.32	**1**	**0.02**
Open inlever	0.268	0.74	0.28	0.41	0.35
Close inlever	0.899	0.83	0.2	0.39	0.39

Bold variables are those that show significant phylogenetic signal, ones in italic show significant sexual dimorphism.

Table 2 Results of a factor analysis performed on the independent contrasts of the morphological data.

	Females Factor 1	Factor 2	Males Factor 1	Factor2
Eigenvalue	5.04	1.79	4.88	1.92
% variation	72.04	25.6	69.69	27.41
Head length	**0.93**	0.31	**0.99**	−0.11
Head width	**0.81**	0.54	**0.97**	0.07
Head height	**0.90**	0.39	**0.96**	0.10
Lower jaw length	**0.92**	0.39	**0.98**	−0.15
Outlever	**0.92**	0.39	**0.99**	−0.10
Snout length	**0.97**	0.22	**0.94**	−0.32
Close inlever	0.30	**0.95**	0.69	**0.70**

Loadings > 0.7 are in bold.

Determinants of bite performance

Females

A factor analysis performed on the independent contrasts of the head dimensions extracted two factors that jointly explained 97% of the variance in the data. Whereas the first factor was principally determined by the independent contrasts of most of the head dimensions, the second factor was principally determined by the independent contrast of the jaw-closing inlever (Table 2). A factor analysis performed on the muscle m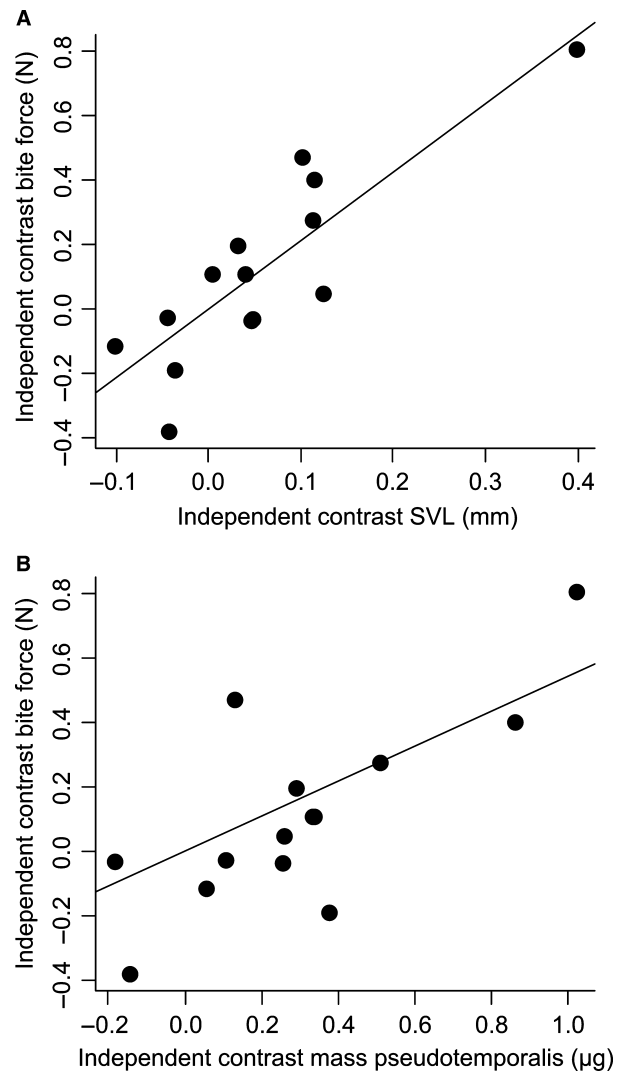ass data extracted two factors that together explained 94% of the variance in the dataset. Whereas the first factor was principally determined by the independent contrasts of the mass of the AMEM, the AMP, PSTP and the PTM, the second factor was determined by the independent contrasts of other muscles (Table 3). Finally, a factor analysis performed on the muscle fibre

Table 3 Results of a factor analysis performed on the independent contrasts of the muscle mass data.

	Females Factor 1	Factor 2	Males Factor 1	Factor2
Eigenvalue	4.51	4.03	4.37	4.13
% variation	50.16	44.80	48.50	45.87
AMESA	0.48	**0.85**	**0.79**	0.62
AMESP	0.68	**0.70**	0.67	**0.70**
AMEM	**0.81**	0.56	**0.74**	0.63
AMEP	0.66	0.69	0.65	**0.73**
AMP	**0.82**	0.56	**0.82**	0.54
PSTS	0.40	**0.87**	0.36	**0.91**
PSTP	**0.89**	0.39	**0.92**	0.37
PTL	0.65	**0.74**	0.62	**0.72**
PTM	**0.82**	0.50	0.57	**0.74**

Loadings > 0.7 are in bold.

Table 4 Results of a factor analysis performed on the independent contrasts of the muscle fibre length data.

	Females		Males	
	Factor 1	Factor 2	Factor 1	Factor2
Eigenvalue	4.58	3.77	4.66	4.28
% variation	50.92	41.88	51.81	47.60
AMESA	**0.75**	0.61	0.65	**0.76**
AMESP	0.44	**0.88**	**0.74**	0.67
AMEM	**0.87**	0.39	**0.73**	0.68
AMEP	**0.90**	0.40	**0.77**	0.63
AMP	0.36	**0.90**	**0.75**	0.66
PSTS	**0.77**	0.58	**0.74**	0.67
PSTP	**0.72**	0.60	0.69	**0.72**
PTL	0.54	**0.81**	**0.75**	0.66
PTM	**0.86**	0.37	0.64	**0.76**

Loadings > 0.7 are in bold.

length data extracted two factors that together explained 92% of the variance in the dataset. Whereas the first factor was determined by the independent contrasts of the fibre lengths of most muscles, factor two was determined by the independent contrasts of the length of the fibres of the AMESP, the AMP and the PTL (Table 4, Fig. 4).

A multiple regression with the factors scores summarizing variation in the independent contrasts of head dimensions, muscle mass and muscle length retained a significant model explaining 91% of the variation in the independent contrasts of bite force ($R^2 = 0.91$; $P = 0.009$). Snout–vent length ($\beta = 1.36$) and the two muscle mass factors ($\beta = 1.57$ and $\beta = 1.23$) positively impacted bite force, with the first muscle mass factor one (AMEM, AMP, PSTP and PTM) being the best predictor. A multiple regression with the independent contrast data of the muscle groups (mass and PCSA) retained a significant model explaining 81% of the variation in the independent contrasts of bite force ($R^2 = 0.81$; $P = 0.026$). Inspection of the standardized partial regression coefficients showed that bite force was positively impacted by the cross-sectional area of the external adductor group ($\beta = 1.03$) and the pterygoideus group ($\beta = 1.62$) as well as by the mass of the pseudotemporalis group ($\beta = 4.63$), the latter being the best predictor of bite force.
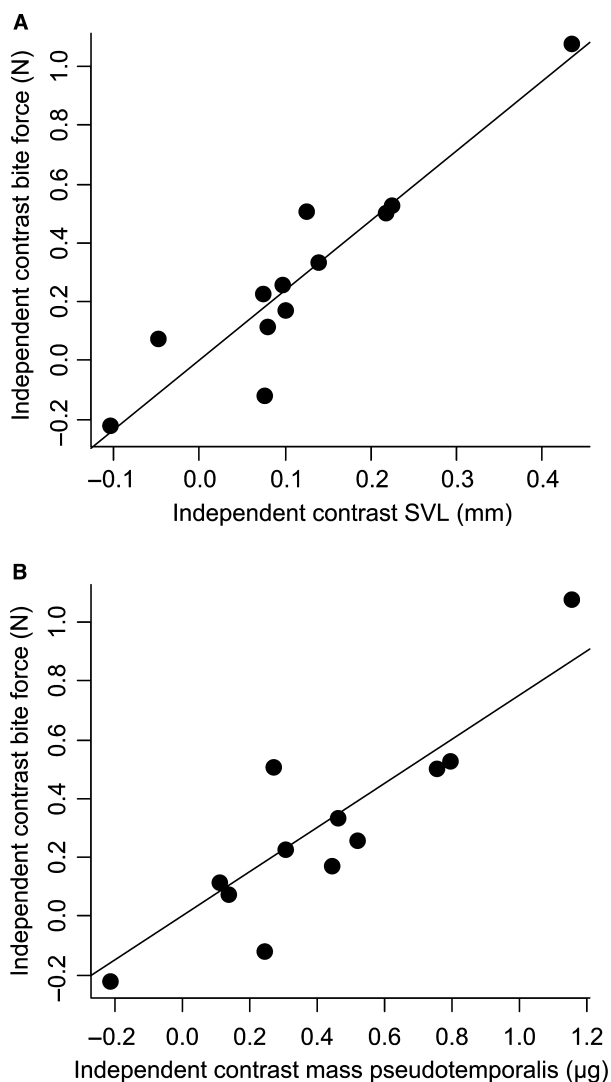
Males

A factor analysis performed on the independent contrasts of the head dimensions extracted two factors that jointly explained 97% of the variance in the data. Whereas the first factor was principally determined by the independent contrasts of most of the head dimensions, the second factor was principally determined by the independent contrast of the jaw-closing inlever (Table 2). A factor analysis performed on the muscle mass data extracted two factors that together explained 94% of the variance in the dataset. Whereas the first factor was principally determined by the

Fig. 4 Scatter plot of the independent contrasts of snout–vent length (A) and the independent contrasts of the mass of the pseudotemporalis muscle (B) against the independent contrasts of bite force for females. Note that the regression line passes through zero.

independent contrasts of the mass of the AMESA, the AMEM, the AMP and the PSTP, the second factor was determined by the independent contrasts of other muscles, with the exception of the AMEP, which loaded equally high on both factors (Table 3). Finally, a factor analysis performed on the muscle fibre length data extracted two factors that jointly explained 99% of the variance in the dataset. Whereas the first factor was determined by the independent contrasts of the fibre lengths of most muscles, factor two was determined by the independent contrasts of the length of the fibres of the AMESA, the PSTP and the PTM (Table 4, Fig. 5).

A multiple regression with the factors scores summarizing variation in the independent contrasts of head dimensions, muscle mass, and muscle length retained a significant

Fig. 5 Scatter plot of the independent contrasts of snout–vent length (A) and the independent contrasts of the mass of the pseudotemporalis muscle (B) against the independent contrasts of bite force for males. Note that the regression line passes through zero.

model explaining 92% of the variation in the independent contrasts of bite force ($R^2 = 0.92$; $P = 0.048$). Snout–vent length ($\beta = 1.47$) and the second muscle mass factor ($\beta = 0.007$; determined by the mass of the AMESP, AMEP, PSTS, PTL and PTM) positively impacted bite force with snout–vent length being the best predictor. A multiple regression with the independent contrast data of the muscle groups (mass and PCSA) retained a significant model explaining 89% of the variation in the independent contrasts of bite force ($R^2 = 0.89$; $P = 0.026$). Inspection of the standardized partial regression coefficients showed that bite force was positively impacted by the cross-sectional area of the external adductor group ($\beta = 2.47$) and the pterygoideus group ($\beta = 1.60$), as well as by the mass of the pseudotemporalis group ($\beta = 3.93$), the latter being the best predictor of bite force.

Discussion

Unexpectedly, some muscles were absent in some species. Specifically, the m. cervicomandibularis appears to be absent in both sexes for island species. In mainland species, this muscle appears to be absent only in males of two species (*A. auratus* and *A. humilis*). These species belong to the *Norops* clade (Pinto et al. 2008), which has Caribbean anole ancestors and originated as the result of a back-colonization from the Greater Antilles to the mainland (Nicholson et al. 2012). As such, this muscle may be of systematic interest. Nevertheless, the presence or absence of this muscle remains to be verified in a larger sample of species of *Anolis* before definitive conclusions can be drawn.

Bite force is generally tightly linked to body size; the bigger an animal is, the harder it bites (Herrel et al. 2001a,b; Aguirre et al. 2002; Herrel et al. 2002; Lailvaux et al. 2004; Vanhooydonck et al. 2005a,b; Lailvaux & Irschick, 2007; Measey et al. 2009; Herrel et al. 2010). This last assumption is in accordance with our results that show that for female *Anolis*, overall body size is among the best predictors of bite performance. The territories of female anoles are mainly determined by availability of food (Andrews, 1971; Fleming & Hooker, 1975; Schoener & Schoener, 1982) and intra-specific competition is generally weak. As such, the main selective pressure acting upon bite force in females is diet. Being able to consume a large range of prey is likely to be linked to survival for two main reasons, first, to avoid starvation when the availability of prey is low, and second, because high bite forces may minimize foraging and feeding time (Verwaijen et al. 2002) and therefore exposure to predation. Thus, the evolution of a larger body size and higher bite forces may allow females to feed on a wider range of prey, including bigger and harder to crush prey types.

Our results show, however, that female anoles that bite harder also have large muscles. Specifically, the mass of the AMEM, AMP, PSTP and PTM strongly impacted bite force. Interestingly, these are all jaw muscles that are positioned deep in the head, close to the brain case. Given that females have narrower heads than males (Table 1) and smaller adductor chambers (Herrel et al. 2007a; Kaliontzopoulou et al. 2007; Ljubisavljević et al. 2010; Fabre et al. 2014a,b) the more laterally positioned muscles such as the superficial external adductor and superficial pseudotemporalis are likely constrained in size, which in turn may explain the importance of the deeper jaw adductors in driving variation in bite force. Our regression model with only muscular traits showed similar results with all three major muscle groups impacting bite force. Specifically, the cross-sectional area of the external adductor and pterygoideus in addition to the mass of the pseudotemporalis were the traits that impacted bite force. The fact that mass rather than cross-sectional area was important for the pseudotemporalis may be explained by the fact that this muscle is parallel-fibred and has relatively long muscle fibres. As such, its overall vol-

ume is likely the trait that drives variation in bite force. As the other muscle groups are pennate with shorter fibres, their overall volume is likely not representative of their cross-sectional area and thus force-generating capacity.

In males, snout–vent length was the best predictor of bite force in our multiple regression model, suggesting that size plays an important role in determining overall bite force in males as it does in females. In addition, the mass of AMESP, AMEP, PSTS, PTL and PTM was important and determined bite force. Rather than being restricted to deep muscles, in males superficial muscles such as the AMESP, the PSTS, or the PTL were also determinants of bite force. In males of many lizard species the superficial jaw adductors such as the AMESP and the PTL are especially well developed and have even been suggested to function as visual signals in the context of male–male combat (Herrel et al. 1999; Huyghe et al. 2005; Fabre et al. 2014a,b) and/or female choice (Cooper & Vitt, 1993). This, moreover, ties in with the fact that in anoles and many other lizards, males have wider heads than females (e.g. Vincent & Herrel, 2007). Indeed, in addition to being subjected to natural selection (i.e. selection imposed by diet; Schoener, 1967; Slatkin, 1984) males are subjected to strong sexual selection. Male *Anolis* often engage in agonistic interactions that sometimes escalate into fights (Jenssen et al. 2005). Fights consist of aggressive biting of a rival, and males with a higher bite force are known to be more successful in fights against other males (Lailvaux et al. 2004; Lailvaux & Irschick, 2007). Moreover, males engage in head-locking behaviour when fighting (Lailvaux et al. 2004). Although the traits that determine bite force in males and females are globally similar, in males the mass of the pseudotemporalis was the best predictor of bite force when examining correlations between muscles and bite force only. This is in accordance with our prediction that muscles with long fibres that are well positioned to generate bite force at large gapes should be important in males. However, this was also the case in females; therefore this cannot be interpreted as the result of selection on males for biting at large gape in the context of male–male combat. The only difference between males and females was that the regression models in males systematically explained a higher proportion of the variation in bite force compared with females, especially for the model based on muscle data only (81 vs. 89%). This suggests that cranial morphology in males may be under stronger selection to generate bite force given that biting in males is important in both feeding and male–male interactions. Clearly, field studies quantifying selection on bite force in males and females are the only way to test this hypothesis.

As a final note, our dataset contained species inhabiting a variety of habitats as well as species from islands as well as the mainland. Although not the goal of our study, it would be of interest to test for differences in muscle size and structure among ecomorphs of the Greater Antilles, given that known differences in head shape exist between ecomorphs (Harmon et al. 2005; Langerhans et al. 2006). Similarly, it would be interesting to test for differences between mainland and island *Anolis* lizards given the known differences in prey size, mainland lizards typically eating relatively larger prey (Andrews, 1979; see also Losos, 2009 for an overview).

References

Aguirre LF, Herrel A, Van Damme R, et al. (2002) Ecomorphological analysis of trophic niche partitioning in a tropical savannah bat community. *Proc Biol Sci* **269**, 1271–1278.

Anderson RA, Vitt LJ (1990) Sexual selection versus alternative causes of sexual dimorphism in teiid lizards. *Oecologia* **84**, 145–157.

Anderson R, Mcbrayer LD, Herrel A (2008) Bite force in vertebrates: opportunities and caveats for use of a nonpareil whole-animal performance measure. *Biol J Linn Soc* **93**, 709–720.

Andrews RM (1971) Structural habitat and time budget of a tropical *Anolis* lizard. *Ecology* **52**, 262–270.

Andrews RM (1979) Evolution of life histories: a comparison of *Anolis* lizards from matched island and mainland habitats. *Breviora* **454**, 1–51.

Barros FC, Herrel A, Kohlsdorf T (2011) Head shape evolution in Gymnophthalmidae: does habitat use constrain the evolution of cranial design in fossorial lizards? *J Evol Biol* **24**, 2423–2433.

Butler M, Losos J (2002) Multivariate sexual dimorphism, sexual selection, and adaptation in Greater Antillean *Anolis* lizards. *Ecol Monogr* **72**, 541–559.

Castaneda MDR, De Queiroz K (2013) Phylogeny of the dactyloa clade of Anolis lizards: new insights from combining morphological and molecular data. *Bull Mus Comp Zool* **160**, 345–398.

Chazeau C, Marchal J, Hackert R, et al. (2013) Proximate determinants of bite force capacity in the mouse lemur. *J Zool* **290**, 42–48.

Cooper WE, Vitt LJ (1993) Female mate choice of large male broad-headed skinks. *Anim Behav* **45**, 683–693.

Diaz-Uriarte R, Garland T Jr (1998) Effects of branch length errors on the performance of phylogenetically independent contrasts. *Syst Biol* **47**, 654–672.

Fabre A-C, Andrade DV, Huyghe K, et al. (2014a) Interrelationships between bones, muscles, and performance: biting in the lizard *Tupinambis merianae*. *Evol Biol* **41**, 518–527.

Fabre A-C, Cornette R, Huyghe K, et al. (2014b) Linear versus geometric morphometric approaches for the analysis of head shape dimorphism in lizards. *J Morphol* **275**, 1016–1026.

Felsenstein J (1985) Phylogenies and the comparative method. *Am Nat* **125**, 1–15.

Fleming TH, Hooker RS (1975) *Anolis cupreus*: the response of a lizard to tropical seasonality. *Ecology* **56**, 1243–1261.

Grafen A (1989) The phylogenetic regression. *Phil Trans R Soc Lond B* **326**, 119–157.

Haas G (1973) Muscles of the jaws and associated structures in the Rhynchocephalia and Squamata. In: *Biology of the Reptilia*, vol. **4** (eds Gans C, Parsons T), pp. 285–490. London: Academic Press.

Harmon LJ, Kolbe JJ, Cheverud JM, et al. (2005) Convergence and the multidimensional niche. *Evolution* **59**, 409–421.

Herrel A, Holanova V (2008) Cranial morphology and bite force in *Chamaeleolis* lizards – adaptations to molluscivory? *Zoology* **111**, 467–475.

Herrel A, O'Reilly JC (2006) Ontogenetic scaling of bite force in lizards and turtles. *Physiol Biochem Zool* **79**, 31–42.

Herrel A, Van Damme R, De Vree F (1996) Sexual dimorphism of head size in *Podarcis hispanica atrata*: testing the dietary divergence hypothesis by bite force analysis. *Netherlands J Zool* **46**, 253–262.

Herrel A, Aerts P, De Vree F (1998) Ecomorphology of the lizard feeding apparatus: a modelling approach. *Netherlands J Zool* **48**, 1–25.

Herrel A, Spithoven L, Van Damme R, et al. (1999) Sexual dimorphism of head size in *Gallotia galloti*: testing the niche divergence hypothesis by functional analyses. *Funct Ecol* **13**, 289–297.

Herrel A, De Grauw E, Lemos-Espinal JA (2001a) Head shape and bite performance in xenosaurid lizards. *J Exp Zool* **290**, 101–107.

Herrel A, Van Damme R, Vanhooydonck B, et al. (2001b) The implications of bite performance for diet in two species of lacertid lizards. *Can J Zool* **79**, 662–670.

Herrel A, O'Reilly JC, Richmond AM (2002) Evolution of bite performance in turtles. *J Evol Biol* **15**, 1083–1094.

Herrel A, Vanhooydonck B, Joachim R, et al. (2004) Frugivory in polychrotid lizards: effects of body size. *Oecologia* **140**, 160–168.

Herrel A, Joachim R, Vanhooydonck B, et al. (2006) Ecological consequences of ontogenetic changes in head shape and bite performance in the Jamaican lizard *Anolis lineatopus*. *Biol J Linn Soc* **89**, 443–454.

Herrel A, McBrayer LD, Larson PM (2007a) Functional basis for sexual differences in bite force in the lizard *Anolis carolinensis*. *Biol J Linn Soc* **91**, 111–119.

Herrel A, Schaerlaeken V, Meyers JJ, et al. (2007b) The evolution of cranial design and performance in squamates: consequences of skull-bone reduction on feeding behavior. *Integr Comp Biol* **47**, 107–117.

Herrel A, Schaerlaeken V, Moravec J, et al. (2009) Sexual shape dimorphism in Tuatara. *Copeia* **4**, 727–731.

Herrel A, Moore JA, Bredeweg EM, et al. (2010) Sexual dimorphism, body size, bite force and male mating success in tuatara. *Biol J Linn Soc* **100**, 287–292.

Huey RB, Stevenson RD (1979) Integrating thermal physiology and ecology of ectotherms: a discussion of approaches. *Am Zool* **19**, 357–366.

Huyghe K, Vanhooydonck B, Scheers H, et al. (2005) Morphology, performance and fighting capacity in male lizards, *Gallotia galloti*. *Funct Ecol* **19**, 800–807.

Irschick DJ, Vanhooydonck B, Herrel A, et al. (2005) Intraspecific correlations among morphology, performance and habitat use within a green anole lizard (*Anolis carolinensis*) population. *Biol J Linn Soc* **85**, 211–221.

Ives AR, Midford PE, Garland JRT (2007) Within-species variation and measurement error in phylogenetic comparative biology. *Syst Biol* **56**, 252–270.

Jackman TR, Larson A, de Queiroz K, et al. (1999) Phylogenetic relationships and tempo of early diversification in *Anolis* lizards. *Syst Biol* **48**, 254–285.

Jenssen T, Decourcy K, Congdon J (2005) Assessment in contests of male lizards (*Anolis carolinesis*): how should smaller males respond when size matters? *Anim Behav* **69**, 1325–1336.

Kaliontzopoulou A, Carretero MA, Llorente GA (2007) Multivariate and geometric morphometrics in the analysis of sexual dimorphism variation in *Podarcis* lizards. *J Morphol* **268**, 152–165.

Kohlsdorf T, Grizante MB, Navas CA, et al. (2008) Head shape evolution in Tropidurinae lizards: does locomotion constrain diet? *J Evol Biol* **21**, 781–790.

Lailvaux SP, Irschick DJ (2007) The evolution of performance-based male fighting ability in Caribbean *Anolis* lizards. *Am Nat* **170**, 573–586.

Lailvaux SP, Herrel A, Vanhooydonck B, et al. (2004) Performance capacity, fighting tactics and the evolution of life-stage male morphs in the green anole lizard (*Anolis carolinensis*). *Proc R Soc B* **271**, 2501–2508.

Langerhans RB, Knouft JH, Losos JB (2006) Shared and unique features of diversification in Greater Antillean *Anolis* ecomorphs. *Evolution* **60**, 362–369.

Lappin AK, Husak JF (2005) Weapon performance, not size, determines mating success and potential reproductive output in the collared lizard (*Crotaphytus collaris*). *Am Nat* **166**, 426–436.

Lappin A, Hamilton PS, Sullivan BK (2006) Bite force performance and head shape in a sexually dimorphic crevice-dwelling lizard, the common chuckwalla [*Sauromalus ater* (=*obesus*)]. *Biol J Linn Soc* **88**, 215–222.

Leal M, Rodríguez-Robles JA (1995) Antipredator responses of *Anolis cristatellus* (Sauria: Polychrotidae). *Copeia* **1995**, 155–161.

Ljubisavljević K, Urosević A, Aleksić I, et al. (2010) Sexual dimorphism of skull shape in a lacertid lizard species (*Podarcis* spp., *Dalmatolacerta* sp., *Dinarolacerta* sp.) revealed by geometric morphometrics. *Zoology* **113**, 168–174.

Losos JB (2009) *Lizards in an Evolutionary Tree: Ecology and Adaptative Radiation of Anoles*. Oakland: University of California Press, Berkeley, CA, USA.

Losos J, Jackman T, Larson A, et al. (1998) Contingency and determinism in replicated adaptive radiations of island lizards. *Science* **279**, 2115–2118.

Martins EP, Garland TJr, (1991) Phylogenetic analyses of the correlated evolution of continuous characters: A simulation study. *Evolution* **45**, 534–557.

Measey GJ, Hopkins K, Tolley KA (2009) Morphology, ornaments and performance in two chameleon ecomorphs: is the casque bigger than the bite? *Zoology* **112**, 217–226.

Mendez J, Keys A (1960) Density and composition of mammalian muscle. *Metabolism* **9**, 184–188.

Munoz MM, Crandell KE, Campbell-Staton S, et al. (2015) Multiple paths to aquatic specialisation in four species of Central American *Anolis* lizards. *J Nat Hist* **49**, 1717–1730.

Nicholson KE, Crother BI, Guyer C, et al. (2012) It is time for a new classification of anoles (Squamata: Dactyloidae). *Zootaxa* **3477**, 1–108.

Pinto G, Mahler DL, Harmon LJ, et al. (2008) Testing the island effect in adaptive radiation: rates and patterns of morphological diversification in Caribbean and mainland *Anolis* lizards. *Proc R Soc B* **275**, 2749–2757.

R Core Team (2014). *R: A Language and Environment for Statistical Computing. R Foundation for Statistical Computing.* Vienna: R Foundation for Statistical Computing. Available at: http://www.R-project.org.

Revell LJ (2012) phytools: an R package for phylogenetic comparative biology (and other things). *Methods Ecol Evol* **3**, 217–223.

Sanger TJ, Losos JB, Gibson-Brown JJ (2008) A developmental staging series for the lizard genus *Anolis*: a new system for the integration of evolution, development, and ecology. *J Morphol* **137**, 129–137.

Schoener TW (1967) The ecological significance of sexual dimorphism in size in the lizard *Anolis conspersus*. *Science* **155**, 474–477.

Schoener TW, Schoener A (1982) Intraspecific variation in home-range size in some *Anolis* lizards. *Ecology* **63**, 809–823.

Slatkin M (1984) Ecological causes of sexual dimorphism. *Evolution* **38**, 622–630.

Vanhooydonck B, Herrel A, Van Damme R, et al. (2005a) Does dewlap size predict male bite performance in Jamaican *Anolis* lizards? *Funct Ecol* **19**, 38–42.

Vanhooydonck B, Herrel A, Meyers JJ, et al. (2005b) The relationship between dewlap size and performance changes with age and sex in an *A. carolinensis* lizard population. *Behav Ecol Sociobiol* **59**, 157–165.

Verwaijen D, Van Damme R, Herrel A (2002) Relationships between head size, bite force, prey handling efficiency and diet in two sympatric lacertid lizards. *Funct Ecol* **16**, 842–850.

Vincent SE, Herrel A (2007) Functional and ecological correlates of ecologically-based dimorphisms in squamate reptiles. *Integr Comp Biol* **47**, 172–188.

Williams EE (1983) Ecomorphs, faunas, island size, and diverse end points in island radiations of *Anolis*. In: *Island Radiations of Anolis* (eds Huey RB, Pianka ER, Schoener TW). pp. 326–370, Cambridge: Harvard University Press.

Supporting Information

Additional Supporting Information may be found in the online version of this article:

Table S1. Collection numbers and origin of dissected specimens from the MCZ collection.

Table S2. Abbreviations and names of jaw muscles.

Table S3. Measurements of dissected specimens (mm).

Table S4. Measurements (mm) and bite force (N) of animals caught in the field.

Table S5. Muscle mass (μg).

Table S6. Fibre length (mm).

Table S7. Physiological cross-sectional area (mm^2).